Elucidation of the Mechanism of Supramolecular Chirality Inversion in Bis(zinc porphyrin) by Dynamic Approach Using CD and 1H NMR Spectroscopy

ARTICLE *in* THE JOURNAL OF PHYSICAL CHEMISTRY A · SEPTEMBER 2000

Impact Factor: 2.69 · DOI: 10.1021/jp001722f

3 AUTHORS, INCLUDING:

Victor Borovkov
Tallinn University of Technology
107 PUBLICATIONS **1,960** CITATIONS
SEE PROFILE

Yoshihisa Inoue
Osaka University
577 PUBLICATIONS **14,441** CITATIONS
SEE PROFILE

Elucidation of the Mechanism of Supramolecular Chirality Inversion in Bis(zinc porphyrin) by Dynamic Approach Using CD and ^{1}H NMR Spectroscopy

Victor V. Borovkov,* Juha M. Lintuluoto, and Yoshihisa Inoue*

Inoue Photochirogenesis Project, ERATO, JST, 4-6-3 Kamishinden, Toyonaka-shi, Osaka 560-0085, Japan

Received: May 8, 2000; In Final Form: July 21, 2000

Dynamic CD and ^{1}H NMR spectroscopies have been applied for studying the phenomenon of chirality inversion in the supramolecular system consisting of bis(Zn porphyrin) and (*R*)-amine upon stepwise titration with (*S*)-amine. The initially induced CD signals corresponding to the coupled B transitions of bis(Zn porphyrin) are gradually decreased during this process and transformed into its mirror images that are the Cotton effects with the same extrema positions, but with opposite signs. In the ^{1}H NMR spectra of this system upon titration there is inversion of the proton signals which are in close proximity to the neighboring porphyrin plane, and are thus the most affected by its ring current effect. The observed spectral changes are caused by shifting of the equilibrium from the left- to right-handed screw in bis(Zn porphyrin) upon titration with the amine of the opposite absolute configuration. The CD and ^{1}H NMR experiments used to determine the reaction kinetics explicitly corroborate each others results. This chirality inversion process has no total energy change ($\Delta G° = 0$), as shown by the titration curves passing through their zero values at the racemic point of an enantiomeric mixture.

Introduction

Supramolecular chirality induction is widely observed in natural and artificial systems. It not only has significance to the functioning of natural systems, but also has important practical implications for the determination of absolute configuration, asymmetric synthesis and catalysis, and production of molecular devices and new materials.[1] This phenomenon arises from conformational changes in achiral chromophoric hosts upon non covalent interactions with chiral guests (and vice versa). Such changes produce asymmetry resulting in optically active electronic transitions of the initially optically inactive chromophores which can be detected in the newly formed supramolecular assembly. In other words, this process can be described as the transfer of asymmetry information from a single element to the whole supramolecular system. Generally, symmetry breaking of an achiral component of a supramolecular assembly upon interaction with either enantiopure guest, yields an enantiomeric structure which is a mirror image of that obtained upon interaction with the opposite enantiomer. For example, an (*S*)-guest may produce a right-handed screw in the achiral host, while an (*R*)-guest results in a left-handed screw (Figure 1, pathways a and b, respectively). So far, this process has been intensively investigated using various supramolecular systems and different spectral methods.[2] Although most spectroscopic techniques can provide enough realistic information regarding the conformational changes in achiral hosts and screw formation, they cannot usually distinguish between the resulting enantiomeric structures because of their similar physicochemical properties. Only circular dichroism (CD) spectroscopy is able to differentiate the corresponding right- and left-handed screws. Based on the general principles of CD spectroscopy[3] one can expect to obtain exact mirror images of the spectral profiles with the opposite signs for different enantiomers. In the case of bi- or multichromophoric systems the absolute configuration of the asymmetric center can be also derived from the signs of CD couplets, according to the CD exciton coupling method.[4]

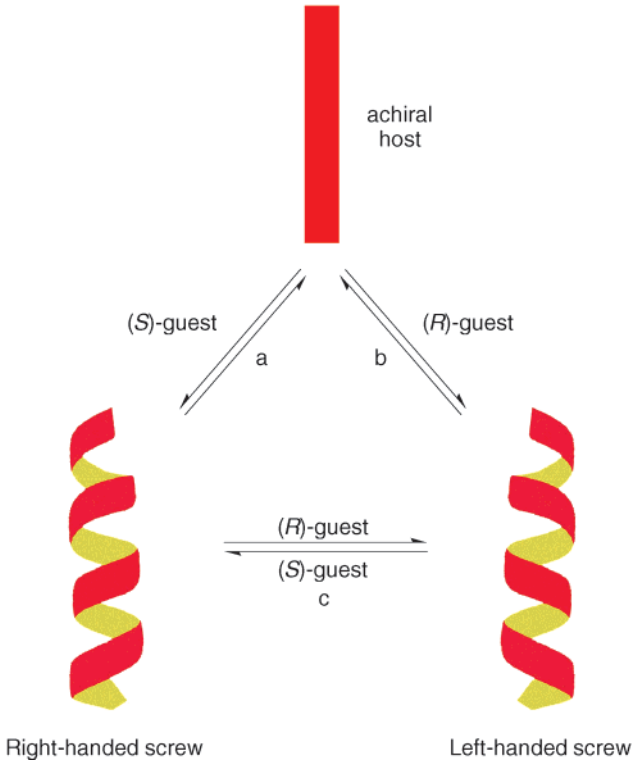

Figure 1. Supramolecular chirality induction (pathways a and b) and inversion (pathway c) via conformational changes in achiral host produced by noncovalent interactions with chiral guests.

However, conventional static spectroscopies cannot always give sufficient information on the dynamics of the chirality transfer processes, which is crucial for comprehensive, in-depth

* Authors to whom correspondence should be addressed. E-mail: victrB@inoue.jst.go.jp.

10.1021/jp001722f CCC: $19.00
Published on Web 09/14/2000

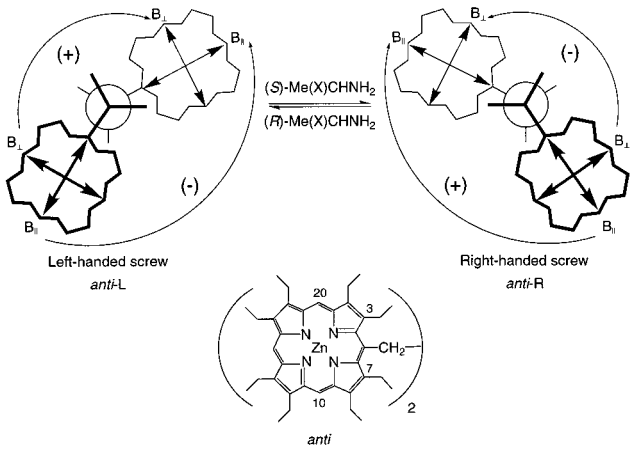

Figure 2. Chiral screw structures, electronic transitions, and mechanism of the supramolecular chirality inversion in bis(Zn porphyrin).

understanding of the mechanism of chiral induction/recognition in supramolecular systems. Therefore, we report here a new approach to studying the stepwise transformation of a left-handed screw into the corresponding right-handed screw (Figure 1, pathway c) by means of dynamic CD and ^{1}H NMR spectroscopies, which gives additional stereochemical information and enables unambiguous assignment of the ^{1}H NMR spectra of the corresponding diastereomers.

Experimental Section

Materials. The syn conformer of the ethane-bridged bis(Zn porphyrin) in which the two porphyrin planes are fixed in a face-to-face orientation was synthesized according to the previously reported methods,[5] and then transformed into the initial *anti*-L form used as the starting material by coordination with the corresponding enantiopure (*R*)-amines (Figure 2).[6] Chiral amines were purchased from Fluka Chemica AG and were used as received. Anhydrous CH_2Cl_2 for UV−vis and CD experiments and $CDCl_3$ for ^{1}H NMR titration measurements were purchased from Aldrich Chemical Co. and used without further purification.

Spectroscopic Measurements. UV−vis and CD spectra were measured at room temperature on a Shimadzu UV-3110PC spectrophotometer and JASCO J-720WI spectropolarimeter, respectively. CD scanning conditions were as follows: scanning rate = 50 nm/min, bandwidth = 1 nm, response time = 0.5 s. The saturated amine concentration used for the static spectral measurements was the concentration where the UV−vis and CD changes were at their maximum and further increase of the amine concentration had no effect on the signal intensities (for the concentration range, see caption of Figure 3).

^{1}H NMR spectra were recorded at 400 MHz on a JEOL JNM-EX 400 spectrometer at 243 K; the low temperature is necessary to maintain an appropriate ratio between the proton peaks of bis(Zn porphyrin) and the proton peaks of the chiral amine by increasing the amine binding strength toward bis(Zn porphyrin) at low temperatures (for the concentration range of the static measurements, see caption of Figure 5). Chemical shifts were referenced to the residual proton resonance in $CDCl_3$ (δ 7.25 ppm).

Titration Experiments. The UV−vis and CD titration experiments were done as follows. A solution of bis(Zn porphyrin) (3 mL, 3.8×10^{-6} M) in CH_2Cl_2 was mixed with a solution of (*R*)-amine (40 μL, 5.7×10^{-1} M) in CH_2Cl_2 in a quartz cell. Portions (10 μL) of a solution of (*S*)-amine (5.7×10^{-1} M) in CH_2Cl_2 were added to the resulting mixture and

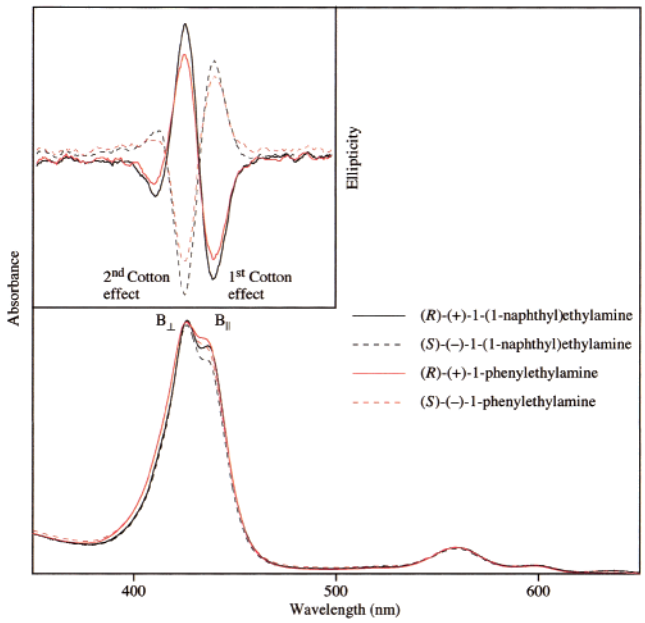

Figure 3. Static UV−vis and CD (inset) spectra of bis(Zn porphyrin) in CH_2Cl_2 containing different chiral amines at 293 K; $C_{bis(Zn\ porphyrin)} = (3.1-3.4) \times 10^{-6}$ M, $C_{amine} = (4.1-5.1) \times 10^{-2}$ M.

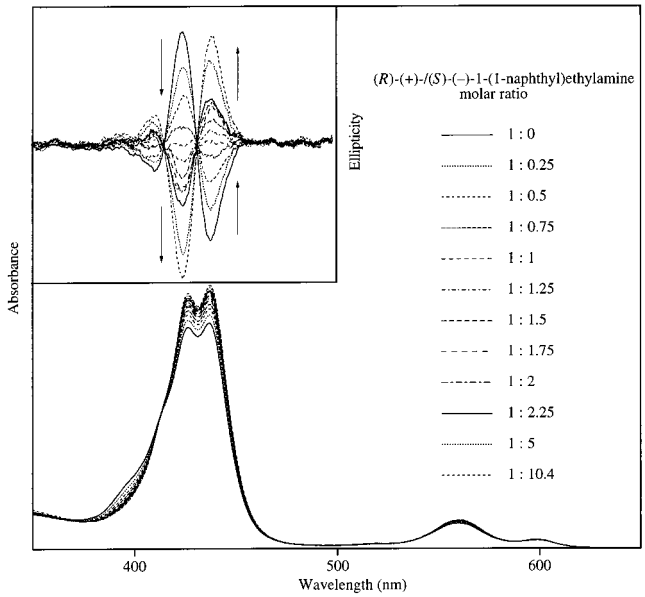

Figure 4. Changes in UV−vis and CD (inset) spectra of the bis(Zn porphyrin)/(*R*)-(+)-1-(1-naphthyl)ethylamine mixture in CH_2Cl_2 ($C_{bis(Zn\ porphyrin)} = 3.8 \times 10^{-6}$ M, $C_{amine} = 7.6 \times 10^{-3}$ M) at 293 K upon titration with (*S*)-(−)-1-(1-naphthyl)ethylamine.

UV−vis and CD spectra were taken after each addition. The obtained spectra were corrected for the decrease of the bis(Zn porphyrin) concentration.

^{1}H NMR titration experiments were done as follows. A solution of bis(Zn porphyrin) (600 μL, 1.5×10^{-3} M) in $CDCl_3$ was mixed with a solution of (*R*)-amine (24 μL, 7.6×10^{-2} M) in $CDCl_3$ in a 5 mm o.d. NMR tube. Portions (6.5 μL) of a solution of (*S*)-amine (7.6×10^{-2} M) in $CDCl_3$ were added to the resulting mixture and ^{1}H NMR spectra were taken after each addition. The monitored $\Delta\delta$ values were corrected for the increase in the total amine concentration.

Results and Discussion

Supramolecular System. Recently we have found that bis(Zn porphyrin)[5] which is connected by a short covalent ethane

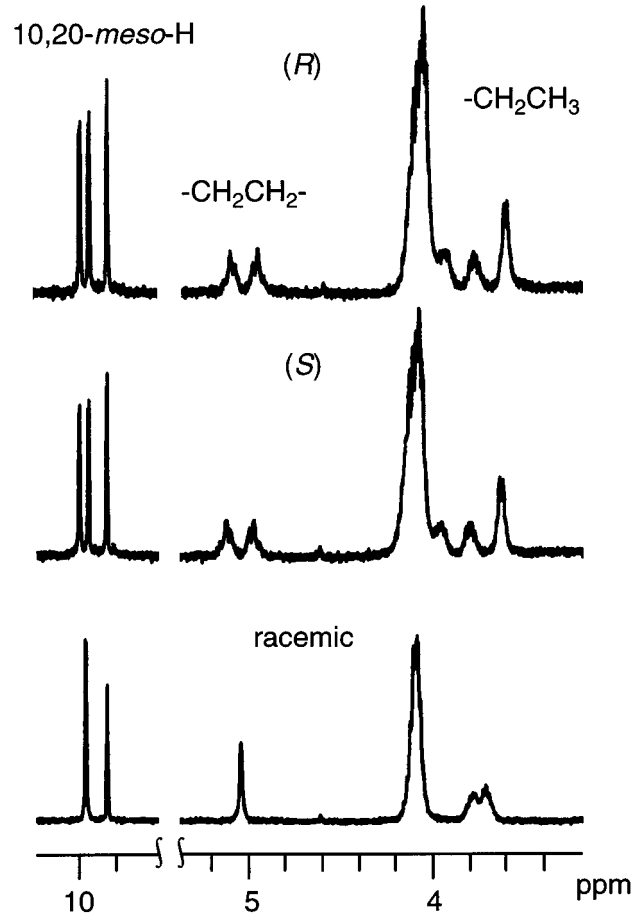

Figure 5. Selected areas of static ^{1}H NMR spectra of bis(Zn porphyrin) in the presence of (*R*)-(+)-1-phenylethylamine (top), (*S*)-(−)-1-phenylethylamine (middle), and racemic 1-phenylethylamine (bottom) in $CDCl_3$ ($C_{bis(Zn\ porphyrin)} = 1.6 \times 10^{-3}$ M, $C_{amine} = 8.0 \times 10^{-3}$ M) at 243 K.

bridge (see the anti structure in Figure 2) is a well-suited host molecule for studying the processes of supramolecular chirality induction.[6] This compound exists in a syn conformation in nonpolar ligand-free solvents due to strong intramolecular $\pi-\pi$ interactions between the two zinc porphyrin macrocycles, while external ligation leads to the conformational switching and formation of the anti form.[7] In the presence of chiral ligands besides syn−anti conformational changes there is another process of structural deformation in bis(Zn porphyrin), resulting in the generation of a screw structure via a steric repulsion mechanism, and hence transformation of point chirality of the guest molecules into supramolecular chirality of the whole system. Since zinc porphyrins are well-known to be five-coordinate species, the ligand approaching from the same side of bis(Zn porphyrin) results in chiral steric interactions between the bulkiest substituent on the asymmetric carbon of the chiral ligand and the ethyl group at either the 3- or 7-position of the neighboring porphyrin ring (depending on the absolute configuration of the ligand), leading to the formation of the screw structure. It was shown that (*S*)-ligands yield the right-handed screw, while (*R*)-ligands give the left-handed screw[6] (see *anti*-L and *anti*-R structures, respectively, in Figure 2).

UV−Vis and CD Spectroscopy. The static UV−vis spectra of bis(Zn porphyrin) in the presence of chiral ligands used in this study at the saturated conditions (see Experimental Section) have the same special feature that is characteristic of the anti form, and reported recently for chiral and achiral amines and alcohols.[6,7] This is a split B (Soret) band (with the $\Delta\lambda$ value ranging from 10 to 13 nm regardless of the ligand type and structure) due to excitonic coupling between the two pairs of the degenerate $B_\perp$ and $B_{||}$ transitions (Davydov split) (Figure 3). These observations are in a good agreement with Kasha's excitonic coupling theory,[8] and such a phenomenon is often seen in UV−vis spectra of bis(porphyrins) in a linear structure where the two porphyrin rings are in an edge-to-edge spatial orientation.[9] For the same class of ligands (for example, amines), the UV−vis spectral pattern of the anti form is almost identical regardless of the ligand's structure.

In contrast to the UV−vis spectra, CD spectral profiles are strongly dependent on the ligand's structure. Static CD spectra of the resulting supramolecular systems contain two major bisignate Cotton effects (Figure 3, inset), which are similar to those described previously.[6] The positions of the first and second Cotton effects are closely matched to the maxima of the split Soret band which are well-resolved in UV−vis spectra, and associated with the allowed $B_{||}$ and $B_\perp$ electronic transitions, respectively. It is assumed that these transitions are the major contributors to the observed CD couplets. Although bi- or multichromophoric systems which are arranged in a chiral spatial orientation, are normally expected to exhibit bisigned CD couplets due to excitonic coupling between their electronic transitions,[1o−u,10] there are only a few examples[11] of such a good match between the CD split (which is determined by the difference of the Cotton effect maxima) and Davydov split in the UV−vis spectrum. It is interesting to note that our supramolecular systems exhibit only moderate splits (694−749 cm^{-1}), while in general this effect is only usually observed when the $\Delta\lambda$ value is relatively large, as in the case of bis-cyanine systems where the energy gap between two exciton bands is as large as 2890 cm^{-1}.[11c]

The signs of the induced CD bands of the supramolecular systems studied are determined by the absolute configuration of the chiral guest, and according to the CD exciton chirality method[4] reflect the spacial orientation of the interacting electronic transition dipoles as described previously.[6] In the case of the left-handed screw of *anti*-L formed by (*R*)-ligands the coupling $B_\perp$ transitions form a clockwise twist, while the coupling $B_{||}$ transitions form an anticlockwise twist (Figure 2), which correspond to the positive first and negative second Cotton effects observed experimentally (Figure 3, inset). The situation with the right-handed screw of *anti*-R induced by (*S*)-ligands is exactly opposite to that with the left-handed screw of *anti*-L, giving negative first and positive second Cotton effects.

The amplitude of the CD couplets is directly dependent on the ligand size, with bulkier ligands inducing more intensive CD signals[6] (Figure 3, inset). Therefore, to monitor the screw inversion dynamics most effectively, 1-(1-naphthyl)ethylamine which is the bulkiest ligand among the chiral guests studied, was chosen to carry out the titration experiments. The initial mixture of bis(Zn porphyrin) and (*R*)-1-(1-naphthyl)ethylamine has a 1:2000 molar ratio. For this molar ratio at 293 K about 85% of bis(Zn porphyrin) is in the anti form as determined by UV−vis spectroscopy. The opposite (*S*)-amine was added to the initial mixture in a stepwise manner until the *R*:*S* molar ratio became 1:10.4. By the end of the titration the syn−anti equilibrium is shifted quantitatively to the anti conformation and these changes are clearly seen in the UV−vis spectra (Figure 4). Reflecting the process of this equilibrium shift, the intensity of the split B bands is steadily enhanced upon increasing the

overall amine concentration, which is expected since the syn−anti conformational switching is dependent on the total ligand concentration rather than enantiomeric composition.

Contrary to UV−vis spectroscopy, CD spectroscopy can recognize individual optically active species or an excess of one of them in a mixture of antipodes. Thus, addition of the (*S*)-enantiomer to the initial mixture of bis(Zn porphyrin) and (*R*)-1-(1-naphthyl)ethylamine results in a gradual decrease of the induced Cotton effect intensities associated with formation of *anti*-L (Figure 4, inset). At the equimolar ratio of the mixture of (*R*)- and (*S*)-amines the whole supramolecular system becomes CD inactive. Subsequent stepwise addition of (*S*)-1-(1-naphthyl)ethylamine results in a corresponding increase of new CD signals of opposite signs. The final CD spectrum obtained upon completion of the titration is an exact mirror image of that recorded for the initial mixture. These changes are the result of the equilibrium shift from the left-handed *anti*-L to the right-handed *anti*-R conformer during addition of (*S*)-amine (Figure 2). Since the directions of all the coupling electronic transitions of *anti*-R are diametrically opposed to those of *anti*-L, the induced Cotton effects resulting from the supramolecular system obtained must exhibit the opposite signs. It is also obvious that at the racemic point all these coupling electronic transitions cancel each other, producing a CD inactive mixture.

^{1}H NMR Spectroscopy. To obtain more detailed information on the dynamics of supramolecular chirality inversion ^{1}H NMR spectroscopy was used to investigate this process. Although this method does not explicitly distinguish between the enantiomeric *anti*-R and *anti*-L structures due to the chemical equivalence and the same spacial arrangement of the protons, as stated above, it becomes possible to follow changes in the signal positions of the protons which are in close proximity to the neighboring porphyrin ring, and hence mostly affected by its ring current effect.

Indeed, the spectral pattern of bis(Zn porphyrin) in the presence of (*R*)-amine is identical to that with (*S*)-amine and distinctly different from that in the presence of a racemic mixture of these amines (Figure 5). The most remarkable distinctions in ^{1}H NMR spectra between pure enantiomeric and racemic amines are as follows. In the case of *anti*-L and *anti*-R, the 10- and 20-*meso* protons and $-CH_2CH_2-$ bridge protons are split into two signals (singlets and multiplets, respectively) of equal intensity. The differences between chemical shifts of the 10- and 20-*meso* protons are 0.05 ppm (for (*R*)- and (*S*)-1-phenylethylamine) and 0.10 ppm (for (*R*)- and (*S*)-1-(1-naphthyl)ethylamine). For the $-CH_2CH_2-$ bridge protons the corresponding splits are 0.13 and 0.26 ppm. The nonequivalence of these protons is a result of their different locations with respect to the neighboring porphyrin ring, leading to the different exposure to its ring current effect. Arising from the same effect, the peripheral CH_2CH_3 protons which are in a close proximity to the neighboring porphyrin ring also become nonequivalent, and exhibit several broad multiplets in the region of 4.20−3.48 ppm for 1-phenylethylamine and 4.25−3.31 ppm for 1-(1-naphthyl)ethylamine. In the case of a racemic mixture of the amine studied, the spectrum profile is more simple in comparison to that of enantiopure ligands. There are no splits between the 10- and 20-*meso* proton signals or the $-CH_2CH_2-$ bridge proton signals. Instead, the proton groups show only two corresponding singlets which are located in the middle of the split proton signals caused by the enantiopure amines. This spectral simplification is a result of the formation of an equimolar ratio of *anti*-L and *anti*-R and their fast mutual equilibrium on the ^{1}H NMR time-scale, in which these protons

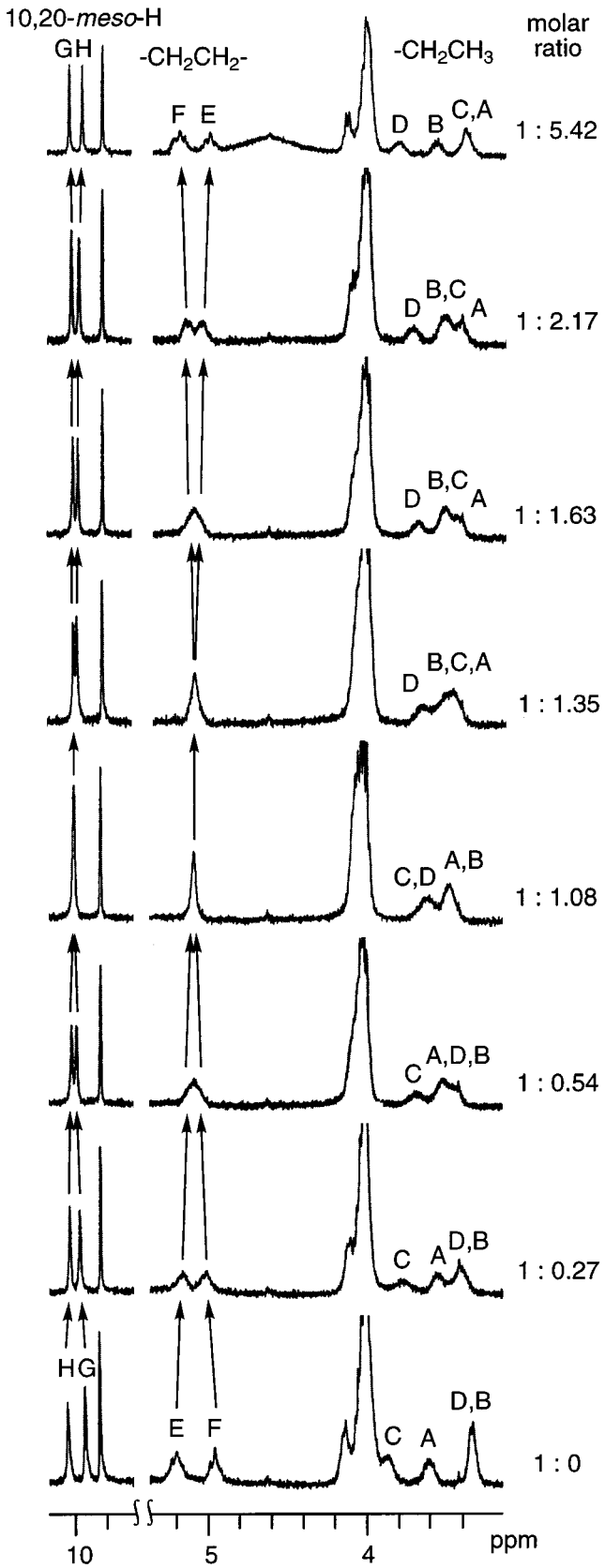

Figure 6. Changes in ^{1}H NMR spectra of the bis(Zn porphyrin)/(*R*)-(+)-1-(1-naphthyl)ethylamine mixture in $CDCl_3$ ($C_{bis(Zn\ porphyrin)}$ = 1.5×10^{-3} M, C_{amine} = 3.0×10^{-3} M) at 243 K upon titration with (*S*)-(−)-1-(1-naphthyl)ethylamine, where molar ratio refers to (*R*)-(+)-/(*S*)-(−)-1-(1-naphthyl)ethylamine.

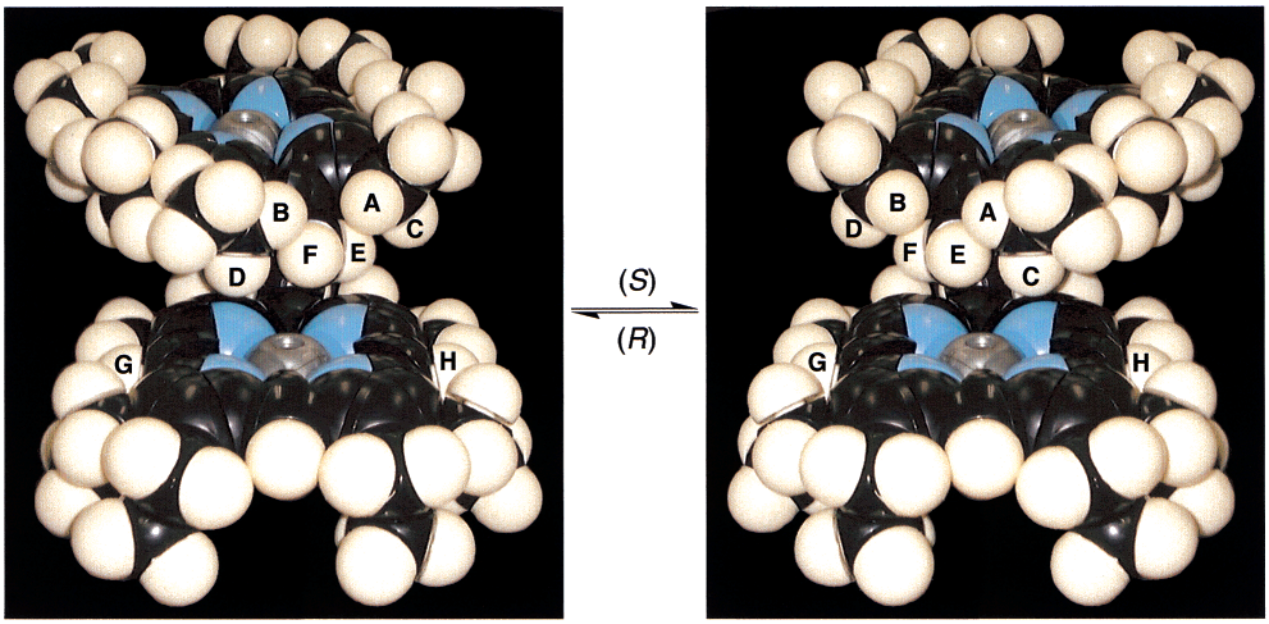

Figure 7. CPK models of the right- and left-handed screws induced in bis(Zn porphyrin) by (*R*)- and (*S*)-amines, respectively.

are exposed equally to both environments (ring current effect of the neighboring porphyrin ring) of *anti*-L and *anti*-R leading to their ^{1}H NMR equivalence.

As with the case of CD spectroscopy, the bulkier ligand gives the more pronounced effect in the ^{1}H NMR spectra (larger signal split), resulting from formation of a greater degree in the screw structure.[6] Therefore, the bulkiest 1-(1-naphthyl)ethylamine has been also chosen for the ^{1}H NMR titration study. The general tendency of the spectral changes upon a stepwise addition of the (*S*)-amine to bis(Zn porphyrin):(*R*)-amine mixture is clearly seen in Figure 6. At the first stage of this process the observed splits between the 10- and 20-*meso* protons and between the $-CH_2CH_2-$ bridge protons are reduced gradually down to zero during addition of the opposite (*S*)-enantiomer and equalization of (*R*)- and (*S*)-amine concentrations. Then, after passing the racemic point the reverse process begins and the observed splits appear again and increase progressively upon further addition. A similar tendency is observed for the CH_2CH_3 protons. Five multiplets come closer together and form three broad signals at the racemic point, followed by movement in the opposite direction producing the final spectral pattern which is much like that as before the titration.

Despite the fact that the initial and final ^{1}H NMR spectra are essentially the same, this close monitoring of the spectral changes allows us to differentiate and assign the magnetic resonances belonging to corresponding pairs of the protons. Particularly, it shows the peak inversion process during addition of the (*S*)-amine resulting in mirror images of the *anti*-L and *anti*-R signals, which obviously originate from the interconversion of the chemical shifts for the corresponding H, G and E, F proton pairs and C, A, D, B protons (the signal movements of the H, G and E, F protons are shown by arrows in Figure 6). The mechanism of the observed peak inversion was aided by interpretation of the spectral data with CPK molecular models of the *anti*-L and *anti*-R structures (Figure 7). In the initial left-handed screw induced by (*R*)-amine the G *meso* protons, F protons of the $-CH_2CH_2-$ bridge, and D, B protons of the CH_2CH_3 group are in the closest proximity to the neighboring porphyrin ring, and hence are the most affected by the ring current effect. This results in appearance of these signals at higher field of the ^{1}H NMR spectrum in comparison to the corresponding H, E, C, and A protons which are farther from the neighboring porphyrin ring. Upon addition of the (*S*)-amine and shifting of the equilibrium to the enantiomeric *anti*-R form with right-handed screw the situation is reversed. The H, E, C, and A protons become closer to the neighboring porphyrin ring and hence their signals are moved upfield. In contrast, the G, F, D, and B protons are moved away from the neighboring porphyrin ring, resulting in the appearance of their resonances at more downfield region. By this mechanism the final spectrum resembles the initial one, but it is clear that the positions of all the signals derived from the above-mentioned pairs of protons are interchanged.

Comparison of CD and ^{1}H NMR Spectral Dynamics. To elucidate the credibility of the spectral methods applied for investigation of the dynamics of chirality inversion in the supramolecular systems studied, the CD and ^{1}H NMR changes have been compared and plotted in Figure 8. To subtract the minor contribution of the syn−anti conformational equilibrium that shifts gradually to the anti form upon addition of the chiral amine (see UV−vis changes in Figure 4), a dissymmetry factor (g) was applied as a monitoring parameter of the CD changes. This is defined as the ratio between CD and unpolarized absorption:

$$g = \Delta\epsilon/\epsilon$$

where $\Delta\epsilon$ is the molar extinction coefficient of the first Cotton effect obtained from the CD spectrum and ϵ is the molar extinction coefficient of the $B_{||}$ transition obtained from the UV−vis spectrum. Since the $B_{||}$ band of the anti conformer is red-shifted in comparison with the B band of the syn conformer by 39 nm and their absorptions are not particularly overlapped, the g value reflects the pure process of chirality inversion caused by the *anti*-R to *anti*-L equilibrium change.

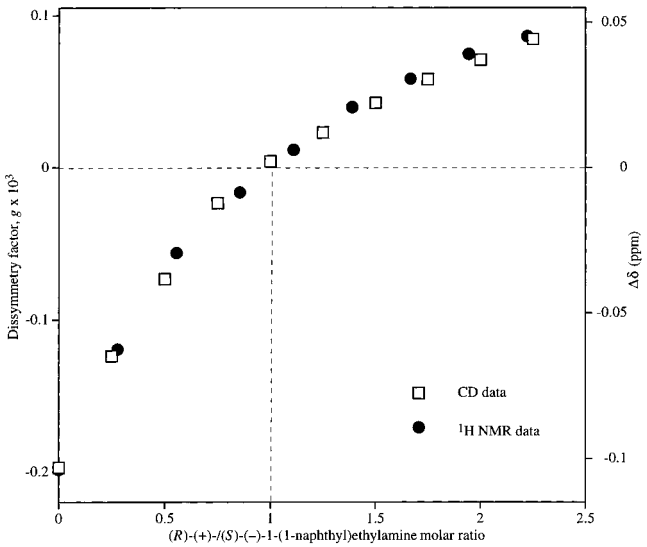

Figure 8. Changes of the dissymmetry factor (g) at the wavelength corresponding to the maximum of the first Cotton effect and B_{II} band, and the corrected chemical shift difference ($\Delta\delta$) between 10- and 20-*meso* protons of the bis(Zn porphyrin):(*R*)-(+)-1-(1-naphthyl)ethylamine mixture upon titration with (*S*)-(−)-1-(1-naphthyl)ethylamine.

For ^{1}H NMR changes the chemical shift difference between the G and H proton signals ($\Delta\delta$) was chosen as a monitoring parameter. It was corrected for the general tendency of these resonances to move in a downfield direction upon the syn to anti equilibrium shift.[6,7] This correction was done on the basis of a titration experiment with a racemic mixture of the corresponding amines, since it shows the nonsplit averaged singlet from both G and H protons.

When the changes of CD and ^{1}H NMR monitoring parameters are plotted versus the molar ratio between the (*R*)- and (*S*)-1-(1-naphthyl)ethylamine it was found that the two sets of experimental data are extremely well matched (Figure 8). Besides this similarity, both titration curves for the g and $\Delta\delta$ parameters pass through their zero values at the racemic point that corresponds to the molar ratio 1:1 of (*R*)- and (*S*)-amines. This means that the chirality inversion process proceeds without a total energy change ($\Delta G^\circ = 0$). Additional confirmation for $\Delta G^\circ = 0$ of this exchange process was obtained from the separate UV−vis and CD titration experiments of bis(Zn porphyrin) with both enantiopure (*R*)- and (*S*)-1-(1-naphthyl)-ethylamine. The ΔG° values for each enantiomer at 293 K are the same and equal −7.7 kcal/mol.[12]

These highly corroborative spectral results obtained independently by CD and ^{1}H NMR spectroscopies reveal that the suggested mechanism of chirality inversion is the most plausible, and that both spectral methods can be successfully applied to studying the processes of asymmetry induction in supramolecular systems.

Conclusion

This work clearly demonstrates that the dynamic approach using CD and ^{1}H NMR spectroscopies can serve as an indispensable technique for studying the mechanisms of asymmetry induction in supramolecular systems, and for solving problems arising from elucidation of the corresponding chiral structures. Particularly, it allows monitoring of the structural changes of bis(Zn porphyrin) leading to the formation of the chiral screw structures, and the unequivocal assignment of specific protons in the ^{1}H NMR spectra of the both enantiomers of bis(Zn porphyrin) complex. This approach should prove to be a powerful tool for the evaluation of chirality induction and asymmetry transfer in various natural and artificial supramolecular assemblies.

Acknowledgment. We thank Dr. G. A. Hembury for assistance in the preparation of this manuscript.

References and Notes

(1) Examples of chirality induction in various supramolecular systems and some possible applications: (a) Meillon, J.-C.; Voyer, N.; Biron, E.; Sanschagrin, F.; Stoddart, J. F. *Angew. Chem., Int. Ed. Engl.* **2000**, *39*, 143−145. (b) Tomooka, K.; Yamamoto, K.; Nakai, T. *Angew. Chem., Int. Ed. Engl.* **1999**, *38*, 3741−3743. (c) Lin, W.; Wang, Z.; Ma, L. *J. Am. Chem. Soc.* **1997**, *119*, 5267−5268. (d) Feringa, B. L.; van Delden, R. A. *Angew. Chem., Int. Ed. Engl.* **1999**, *38*, 3419−3438. (e) Green, M. M.; Park, J.-W.; Sato, T.; Teramoto, A.; Lifson, S.; Selinger, R. L. B.; Selinger, J. V. *Angew. Chem., Int. Ed. Engl.* **1999**, *38*, 3139−3154. (f) Akagi, K.; Piao, G.; Kaneko, S.; Sakamaki, K.; Shirakawa, H.; Kyotani, M. *Science* **1998**, *282*, 1683−1686. (g) Yashima, E.; Maeda, K.; Okamoto, Y. *Nature* **1999**, *399*, 449−451. (h) Prins, L. J.; Huskens, J.; de Jong, F.; Timmerman, P.; Reinhoudt, D. N. *Nature* **1999**, *398*, 498−502. (i) Verbiest, T.; Van Elshocht, S.; Kauranen, M.; Hellemans, L.; Snauwaert, J.; Nuckolls, C.; Katz, T. J.; Persoons, A. *Science* **1998**, *282*, 913−915. (j) Rivera, J. M.; Martin, T.; Rebek, J., Jr. *Science* **1998**, *279*, 1021−1023. (k) Suárez, M.; Branda, N.; Lehn, J.-M.; Decian, A.; Fisher, J. *Helv. Chim. Acta* **1998**, *81*, 1−13. (l) Sakamoto, M. *Chem. Eur. J.* **1997**, *3*, 684−689. (m) Oda, R.; Huc, I.; Schmutz, M.; Candau, S. J.; MacKintosh, F. C. *Nature* **1999**, *399*, 566−569. (n) Jha, S. K.; Cheon, K.-S.; Green, M. M.; Selinger, J. V. *J. Am. Chem. Soc.* **1999**, *121*, 1665−1673. (o) Seifert, J. L.; Connor, R. E.; Kushon, S. A.; Wang, M.; Armitage, B. A. *J. Am. Chem. Soc.* **1999**, *121*, 2987−2995. (p) Smith, J. O.; Olson, D. A.; Armitage, B. A. *J. Am. Chem. Soc.* **1999**, *121*, 2686−2695. (q) Huang, X.; Borhan, B.; Rickman, B. H.; Nakanishi, K.; Berova, N. *Chem. Eur. J.* **2000**, *6*, 216−224. (r) Huang, X.; Rickman, B. H.; Borhan, B.; Berova, N.; Nakanishi, K. *J. Am. Chem. Soc.* **1998**, *120*, 6185−6186. (s) Ogoshi, H.; Mizutani, T. *Acc. Chem. Res.* **1998**, *31*, 81−89. (t) Purrello, R.; Bellacchio, E.; Gurrieri, S.; Lauceri, R.; Raudino, A.; Scolaro, L. M.; Santoro, A. M. *J. Phys. Chem. B* **1999**, *103*, 5151−5156. (u) Yashima, E.; Matsushima, T.; Okamoto, Y. *J. Am. Chem. Soc.* **1997**, *119*, 6345−6359.

(2) (a) Takeuchi, M.; Imada, T.; Shinkai, S. *Angew. Chem., Int. Ed. Engl.* **1998**, *37*, 2096−2099. (b) Mizutani, T.; Yagi, S.; Honmaru, A.; Murakami, S.; Furusyo, M.; Takagishi, T.; Ogoshi, H. *J. Org. Chem.* **1998**, *63*, 8769−8784. (c) Mizutani, T.; Yagi, S.; Honmaru, A.; Ogoshi, H. *J. Am. Chem. Soc.* **1996**, *118*, 5318−5319. (d) Dietrich-Buchecker, C.; Rapenne, G.; Sauvage, J.-P.; De Cian, A.; Fischer, J. *Chem. Eur. J.* **1999**, *5*, 1432−1439.

(3) Nakanishi, K.; Berova, N.; Woody, R. W. *Circular Dichroism: Principles and Applications*, Wiley-VCH: New York, 1994.

(4) Harada, N.; Nakanishi, K. Circular *Dichroic Spectroscopy. Exciton Coupling in Organic Stereochemistry*, University Science Books: Mill Valley, CA, 1983.

(5) (a) Borovkov, V. V.; Lintuluoto, J. M.; Inoue, Y. *Synlett* **1998**, 768−770. (b) Borovkov, V. V.; Lintuluoto, J. M.; Inoue, Y. *Helv. Chim. Acta* **1999**, *82*, 919−934.

(6) (a) Borovkov, V. V.; Lintuluoto, J. M.; Fujiki, M.; Inoue, Y. *J. Am. Chem. Soc.* **2000**, *122*, 4403−4407. (b) Borovkov, V. V.; Lintuluoto, J. M.; Inoue, Y. *Org. Lett.* **2000**, *2*, 1565−1568.

(7) (a) Borovkov, V. V.; Lintuluoto, J. M.; Inoue, Y. *Tetrahedron Lett.* **1999**, *40*, 5051−5054. (b) Borovkov, V. V.; Lintuluoto, J. M.; Inoue, Y. *J. Phys. Chem. B* **1999**, *103*, 5151−5156.

(8) Kasha, M.; Rawls, H. R.; El-Bayoumi, M. A. *Pure Appl. Chem.* **1965**, *11*, 371−392.

(9) (a) Zhou, X.; Chan, K. S. *J. Org. Chem.* **1998**, *63*, 99−104. (b) Chernook, A. V.; Shulga, A. M.; Zenkevich, E. I.; Rempel, U.; von Borczyckowski, C. *J. Phys. Chem.* **1996**, *100*, 1918−1926. (c) Sessler, J. L.; Johnson, M. R.; Lin, T.-Y.; Creager, S. E. *J. Am. Chem. Soc.* **1988**, *110*, 3659−3661.

(10) Examples of chirality induction in various covalently linked bi- and multichromophoric systems: (a) Superchi, S.; Donnoli, M. I.; Rosini, C. *Org. Lett.* **1999**, *1*, 2093−2096. (b) Zahn, S.; Canary, J. W. *Org. Lett.* **1999**, *1*, 861−864. (c) Guiper, A. D.; Brzostowska, M.; Gawronski, J. K.; Smeets, W. J. J.; Spek, A. L.; Hiemstra, H.; Kellogg, R. M.; Feringa, B. L. *J. Org. Chem.* **1999**, *64*, 2567−2570. (d) Chisholm, J. D.; Golik, J.; Krishnan, B.; Matson, J. A.; Van Vranken, D. L. *J. Am. Chem. Soc.* **1999**, *121*, 3801−3802. (e) Gawronski, J.; Gawronska, K.; Skowronek, P.; Holmen, A. *J. Org. Chem.* **1999**, *64*, 234−241. (f) Yamaguchi, T.; Nakazumi, H.; Irie, M. *Bull. Chem. Soc. Jpn.* **1999**, *72*, 1623−1627. (g) Lou, J.; Hashimoto, M.; Berova, N.; Nakanishi, K. *Org. Lett.* **1999**, *1*, 861−864. (h) Iuliano, A.; Voir, I.; Salvadori, P. *J. Org. Chem.* **1999**, *64*, 5754−5756. (i) Liu, H.-y.; Huang, J.-w.; Tian, X.; Jiao, X.-d.; Luo, G.-t.; Ji, L.-n. *Chem. Commun.* **1997**, 1575−1576. (j) Ema, T.; Misawa, S.; Nemugaki,

S.; Sakai, T.; Utaka, M. *Chem. Lett.* **1997**, 487−488. (k) Arai, T.; Takei, K.; Nishino, N.; Fujimoto, T. *Chem. Commun.* **1996**, 2133−2134. (l) Matile, S.; Berova, N.; Nakanishi, K.; Fleischhauer, J.; Woody, R. W. *J. Am. Chem. Soc.* **1996**, *118*, 5198−5206.

(11) Examples of systems with a good match between CD and Davydov splits: (a) Gargiulo, D.; Ikemoto, N.; Odingo, J.; Bozhkova, N.; Berova, N.; Nakanishi, K. *J. Am. Chem. Soc.* **1994**, *116*, 3760−3767. (b) Gargiulo, D.; Cai, G.; Ikemoto, N.; Bozhkova, N.; Odingo, J.; Berova, N.; Nakanishi, K. *Angew. Chem., Int. Ed. Engl.* **1993**, *32*, 888−891. (c) Berova, N.; Gargiulo, D.; Derguini, F.; Nakanishi, K.; Harada, N. *J. Am. Chem. Soc.* **1993**, *115*, 4769−4775.

(12) These data will be reported elsewhere.